INTERNATIONAL JOURNAL OF FLUID POWER, 2017
VOL. 18, NO. 1, 3–16
http://dx.doi.org/10.1080/14399776.2016.1234873

Taylor & Francis
Taylor & Francis Group

Properties and sizing methods of 2-motor transmissions

Roberto Paoluzzi[†] and Luca G. Zarotti

C.N.R.-IMAMOTER Institute for Agricultural and Earthmoving Machines, National Research Council of Italy, Ferrara, Italy

ABSTRACT
The hydrostatic transmissions are often used to operate the drive train of off-road machines (wheeled or tracked) due to their advantages, e.g. compact size, little inertia, wide speed range, dynamic braking. Since the typical transmission with one pump and one motor (named Type A for convenience) features a rather limited application range – i.e. compatibility of specifications in terms of engine power, maximum traction and top speed – the paper reviews three improvementes to expand it without introducing too much complexity: the addition of a gearbox in series (Type B), and two alternative schemes with two motors: fixed and variable (Type C), or both variable (Type D). The constraints on size, setting and speed of the main hydraulic units dictated by each of the configurations are disclosed and their consistent design rules are discussed in detail on the basis of discrete series of heavy duty pumps and motors taken from the technical literature. To highlight the realistic implementation of the transmissions with two motors, the conventional traction vs. speed curves of three Type C and D transmissions are compared by interpolating 2-D and 3-D efficiency tables.

ARTICLE HISTORY
Received 26 December 2015
Accepted 5 September 2016

KEYWORDS
Fluid power; transmissions; off-road machines; volumetric machines

1. Introduction

The users of mobile vehicles such as earth moving machines, agriculture and forest machines, industrial and mining lifters seek the best performance and fluid power systems can offer valuable help to meet this demand. In fact, a multitude of hydraulic circuits are the standard solution to operate the working equipment, whereas the hydrostatic transmission (HT in brief) competes with others or does not compete at all to meet the locomotion requirements, despite its known advantages as: high power capacity in a compact package, addition of little inertia to the total rotating mass, operation over a wide range of output speed without changing the prime mover speed, retention of preset speed against driving or overrunning loads, undamaged stall under full load, intrinsic dynamic braking, faster response than mechanical or electromechanical transmissions of comparable rating.

The choice of a specific transmission balances several figures of merit – engineering, manufacturing, marketing, cost – and the analysis of its performance goes through sophisticated simulation tools; but the preliminary evaluation of its potential can be simplified by accepting the locomotion performance be synthesized by the so called 'power ratio', defined as maximum traction times maximum speed divided by available engine power (Zarotti and Paoluzzi 1996, Paoluzzi and Zarotti 1997, Paoluzzi and Zarotti 2013): as to the HT, the combination of power ratio and engine power determines whether it be feasible or not. A good example is the telehandler or telescopic handler, a versatile machine used in construction, agriculture, industry and mining – a major player in the market, though its birth dates back to the sixties of the past century – whose power ratio is generally between ten and fifteen, sometimes more; until engine power is relatively low (about 40 kW) the transmission is normally hydrostatic, but as power increases the transmission turns to be mechanical of some sort. Since a similar limitation applies to other machines, e.g. wheel loaders, the expansion of the application range is a real challenge to the HT design.

The paper presents four HT schemes of increasing complexity (Type A, B, C and D) to show how the growing demand for enhanced combinations of power ratio and engine power can be satisfied. All transmission schemes share the assumption of a single output shaft, i.e. no wheel motors or similar, and a single power flow from input to output, i.e. no CVT or dual path. Differently from other surveys, e.g. Rydberg (1997), the constitutive models and the sizing methods are explained in detail and illustrated by examples; the most promising Type C and D, in particular, have been met with sympathy in recent years in theory and practice, but the invariable approach found in literature is to present *what* they are, not *why*.

CONTACT Luca G. Zarotti gl.zarotti@imamoter.cnr.it
[†]Roberto Paoluzzi passed away suddenly on September 13th 2016.

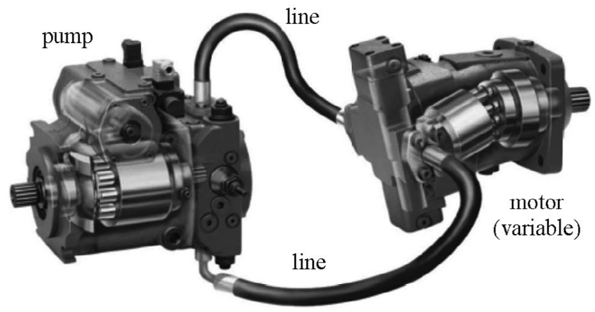

Figure 1. Layout of the Type A transmission.

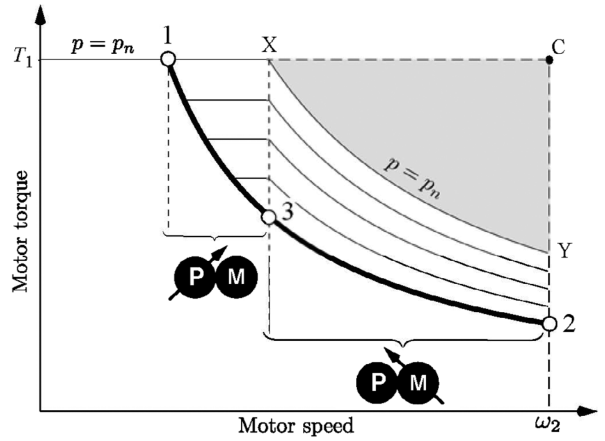

Figure 2. Mechanical characteristic of the Type A transmission.

2. Type A transmission

The simplest but still widely adopted arrangement of the HT has one variable displacement pump and one fixed or variable displacement motor connected by two lines, usually hoses, through which the operating fluid moves at high and low pressure interchangeably; the boost circuit and other auxiliaries, whose description is irrelevant to the subject of the paper, are embedded in the case of the main units (Figure 1).

The pump shaft is connected to the prime mover, usually a diesel engine, through a front drive and the motor shaft to the traction wheels through a final drive. The loss free steady state model of the transmission in the driving mode – power from input to output shaft – is made up of two laws. Assuming the setting of both units be variable,[1] the first law is the flow continuity in the high pressure line

$$\alpha_p D_p \omega_p = Q = \alpha_m D_m \omega_m \tag{1}$$

The second law is the balance of the differential pressure between the lines at the external ports of pump and motor

$$\frac{T_p}{\alpha_p D_p} = p = \frac{T_m}{\alpha_m D_m} \tag{2}$$

The setting of pump and motor are dimensionless variables subject to upper and lower bounds

$$-1 \leq \alpha_p \leq 1 \qquad \alpha_0 \leq \alpha_m \leq 1 \tag{3}$$

The bounds of the pump setting as well as the upper bound of the motor setting are functional and physical; conversely, the minimum setting α_0 is often functional, at least in the so called 'zero motors' that can be switched to $\alpha_m = 0$ and self-locking there (see Appendix 1): a feature used to a some extent in Type B transmissions and to a greater extent in Type C and D. The control of the pump and motor setting normally obeys the 'sequential rule' – α_p changes while α_m is 1, and vice versa – driven by an external command, possibly overrun by one or more automatic actions (the pressure and/or torque limiter are prevalent).

2.1. Properties and size

By fixing the maximum power at the input shaft, the loss free or ideal torque vs. speed curve at the output shaft alias mechanical characteristic alias operating envelope of the transmission is a finite portion of a hyperbola between point 1 of maximum torque and point 2 of maximum speed (Figure 2). The additional assumption of constant pump speed – consistent with current practice – makes the sequential rule applicable through the intermediate point 3:

- From 1 to 3 the pump setting changes from the minimum α_1 to 1, while the motor setting is 1. The differential pressure decreases from the maximum p_n to the lower $p_3 = \alpha_1 p_n$, compatible with higher output speed at constant input power;
- From 3 to 2 the pump setting is 1 (constant flow), while the motor setting decreases from 1 to the minimum $\alpha_2 \geq \alpha_0$. The differential pressure is the same as in point 3 or $p_2 = p_3$ for compatibility with constant pump flow and that's why the constant pressure lines run as hyperbolas.

The corner point C, where $T_m = T_1$ and $\omega_m = \omega_2$, defines the so called 'corner power' and eventually, once divided by the input power, the power ratio of the transmission or internal power ratio (always greater than the power ratio based on the vehicle performance)

$$R_i = \frac{T_1 \omega_2}{P_e} = \frac{1}{\alpha_1 \alpha_2} \tag{4}$$

For a given α_2, the lowest possible R_i occurs at $\alpha_1 = 1$ and the relevant mechanical characteristic corresponds to the constant pressure hyperbola XY; all points of the slice XCY are beyond reach of the transmission.

The size of motor and pump are derived from the continuity and balance law plus the compatibility of point 1, 2 and 3 with the input power $P_e @ \omega_e$ (in general $\omega_p \neq \omega_e$)

$$D_m = \frac{P_e R_i}{\omega_2 p_n} \tag{5}$$

Table 1. Properties of pumps and motors used in the paper.

	ID label*	ϖ	ε	Corner power, kW	α_0
Pumps	78	50.85	0.175	205	–
	100			251	
	130			312	
Motors (V)	60	8.00	0.333	259	0.2**
	80			312	
	110			382	
	160			499	
Motors (F)	55	17.38	0.271	161	–
	75			203	
	100			248	
	130			302	

*Units are usually identified by their cubic displacement in cm^{3}rev^{-1}; **This value applies when the motor works alone.

$$D_p = \frac{\alpha_2 \omega_2}{\omega_p} D_m = \frac{P_e}{\omega_p p_n \alpha_1} \tag{6}$$

Since the transit between point 2 and 3 is only due to the motor setting and consequently $\omega_3 = \alpha_2\omega_2$, the relative ratio of speed range between point 2 and 3, i.e. the motor control range, is

$$\frac{\omega_2 - \omega_3}{\omega_2} = \lambda = 1 - \alpha_2 \tag{7}$$

By taking the couple (R_i, P_e) as input specifications and a pre-specified value for p_n, the nonlinear algebraic system of Equations (4)–(6) with six unknowns $\omega_2, \omega_p, \alpha_1, \alpha_2, D_p, D_m$ is an underdetermined problem and three degrees of freedom have to be removed through additional equations.

2.2. Dimensional data base

The displacement of commercial pumps and motors are arranged in homogeneous series. If the series is not too long, its members share the maximum pressure, whereas their maximum speed at full setting decreases as displacement increases and obeys, with rather good approximation, a power law (Paoluzzi and Zarotti 2013)

$$\omega_n = \varpi D^{-\varepsilon} \tag{8}$$

where ϖ is a constant dependent on design and technology, and the exponent ε is often – not always – close to the theoretical 1/3 from the law of similitude. Furthermore, variable motors are allowed to exceed the maximum speed at partial settings ($\alpha_m < 1$) up to the top speed $\Omega\,\omega_n$ according to a function Ω reasonably simplified as

$$\Omega(\alpha_m) = \min\left\{\alpha_m^{-1}, \Omega_0\right\} \tag{9}$$

where Ω_0 is an absolute upper bound slowly increasing as technology develops; the overspeed does not matter to pumps, constrained as they are by the prime mover. The series of units used in this investigation – variable pumps, variable and fixed motors – and their relevant properties are collected in Table 1; in this case the variable motors have $\Omega_0 = 1.6$.

The maximum working pressure of all units is 45 MPa, which means that they belong to the 'heavy duty' class, so called because it claims the top sophistication and performance among the rotating hydraulic machines for mobile applications.

2.3. Application range

The laws of Equations (8) and (9) help remove two degrees of freedom of the underdetermined system of Equations (4)–(6) if ω_p and ω_2 are expressed in proportion to the maximum speed of pump and top speed of motor, respectively

$$\omega_p = \varphi_p \varpi_p D_p^{-\varepsilon_p} \qquad \omega_2 = \varphi_m \varpi_{mv} D_m^{-\varepsilon_{mv}} \Omega(\alpha_2)$$

where the coefficient φ_{pj} and φ_{mj} (both less or equal to 1 by definition) are adjusted to satisfy the application requirements. The third degree of freedom is removed by a relationship between the minimum setting of pump (α_1) and motor (α_2). A common assumption is that they be balanced or $\alpha_1 = \alpha_2 = 1/\sqrt{R_i}$ which means that $\omega_3/\omega_1 = \omega_2/\omega_3$ (Figure 2); consequently, α_2 is not saturated against α_0 if $R_i \le 25$ and the Ω function saturates above the power ratio $1.6^2 = 2.56$, very low indeed in wheeled machines.

Eventually, the size of the jth variable motor of the series in Table 1 can be written as

$$D_{mj}^{1-\varepsilon_{mv}} = \frac{P_e R_i}{\varphi_{mj} \varpi_{mv} \Omega(\sqrt{R_i}) p_n} \qquad j = 1, \ldots, 4 \tag{10}$$

where $j = 1$ designates the smallest motor and so on. Similarly, the size of the jth pump of the series in Table 1 can be written as

$$D_{pj}^{1-\varepsilon_p} = \frac{P_e \sqrt{R_i}}{\varphi_{pj} \varpi_p p_n} \qquad j = 1, \ldots, 3 \tag{11}$$

where $j = 1$ designates the smallest pump and so on.

The specifications (R_i, P_e) are compatible with the application range of the jth motor or pump if the relevant φ_{mj} or φ_{pj} is within its upper limit; the graphical check is straightforward in the size map of Figure 3 where the upper boundaries of all units are plotted together in a log-log scale. At first sight the application range of the transmission is always decided by the motor, since it dictates the most restrictive condition; in actual fact, the whole grey region is excluded. If, for instance, the specifications correspond to point A, the 160 motor is the only choice (running up to 97% of its top speed); if they correspond to point B, the 80 motor is the minimum size (up to 96% speed) but the 110 and 160 are also possible

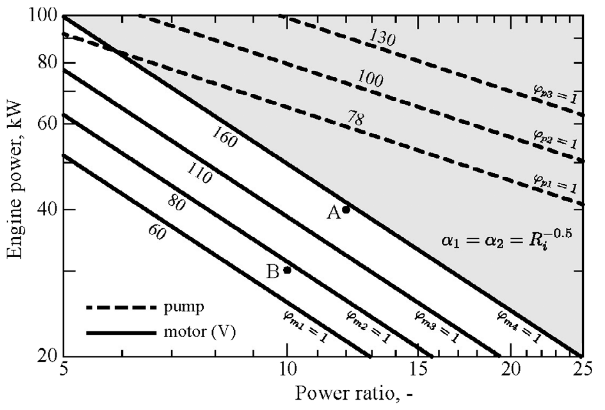

Figure 3. Size map of the Type A transmission with balanced settings.

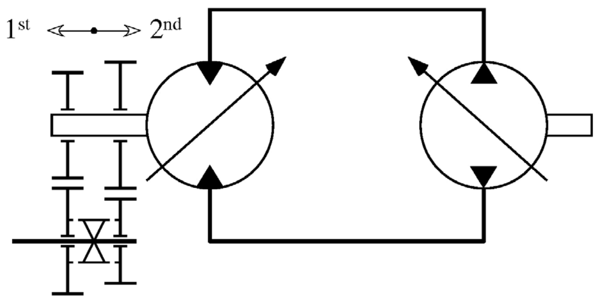

Figure 4. Scheme of the Type B transmission.

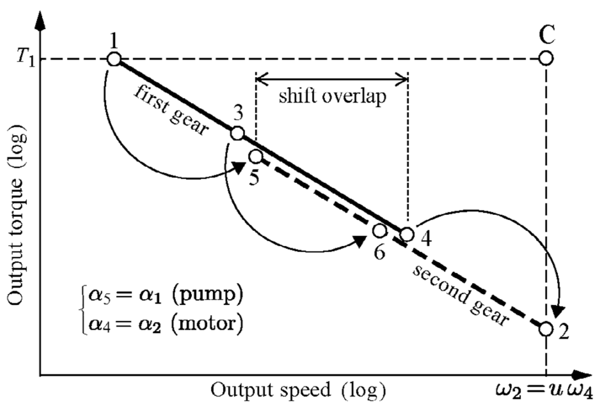

Figure 5. Mechanical characteristic of the Type B transmission (log–log scale).

(up to 77 and 60% speed). As to the pump boundaries, the smallest unit seems always satisfactory apart from the upper left region of the map; to match point A the 78 pump runs at 68% of its maximum speed. As to the practical use of the map, the selection of the transmission units is always conservative because the volumetric efficiency scales back the true speed.

An alternative approach within the same method is to separate the minimum settings, e.g. by fixing λ in Equation (7) which means a constant $\alpha_2 = 1 - \lambda$ and a variable $\alpha_1 = 1/R_i(1 - \lambda)$; λ is often in the range of 0.6 or close to it (to justify the money spent to buy a variable motor). The motor boundaries of the size map (not shown) are as in Figure 3 because Ω is still saturated, while the pump boundaries are all beyond and parallel to the largest motor boundary; for all practical purposes, nothing changes.

3. Type B transmission

According to a settled tradition, the Type B transmission expands the application range of Type A by adding a two step gearbox as in Figure 4, where the boost circuit and other auxiliaries are omitted. If the upshift and downshift are only feasible when the machine has been brought to a standstill, the true power ratio of the assembly is still that of the embedded Type A transmission; conversely, if the upshift and downshift are feasible either manually or automatically when the motor shaft rotates, the true power ratio of the assembly increases. The latter is the only instance considered here.

3.1. Properties and size

Supposed to be 1 the ratio of the first gear and $u > 1$ the ratio of the second gear, the ideal characteristic of the assembly (Figure 5) is the characteristic of the embedded HT plus a translated copy of it in the log-log scale (the vertical gap is just for visibility), where hyperbolas are straight segments; speed and torque are now referred to the output shaft of the gearbox. Since the key points are the same in both pieces of the characteristic ($1 \rightarrow 5$, $3 \rightarrow 6$, $4 \rightarrow 2$) the power ratio comes from Equation (4) as follows

$$R_i = \frac{T_1 \omega_2}{P_e} = \frac{T_1 u \omega_4}{P_e} = \frac{u}{\alpha_1 \alpha_4} \tag{12}$$

Proceeding as in Section 2, the pump size from Equation (6) does not change, while the motor size becomes the following

$$D_m = \frac{P_e R_i}{\omega_4 p_n u} \tag{13}$$

Formally the Type B transmission is equivalent to a Type A transmission with power ratio R_i/u, but with limited freedom. Firstly, u affects the shift overlap ratio δ, i.e. the length of the shift overlap divided by the motor speed in point 2, since the positive overlap of first and second gear is guaranteed if

$$\frac{\omega_4 - \omega_5}{\omega_2} = \delta = \frac{1}{u} - \frac{u}{R_i} > 0 \qquad u < \sqrt{R_i} \tag{14}$$

Secondly, u is constrained by an upper limit u_0 due to the technical properties of the gearboxes (a value $u_0 \approx 3$ is often reported), and δ is constrained by a lower limit due to the shift implementation (redundant in this transmission).

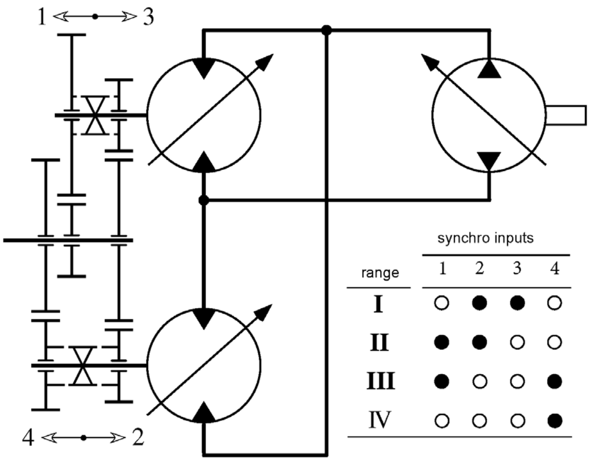

Figure 6. Complex scheme of a transmission with two motors and gearbox.

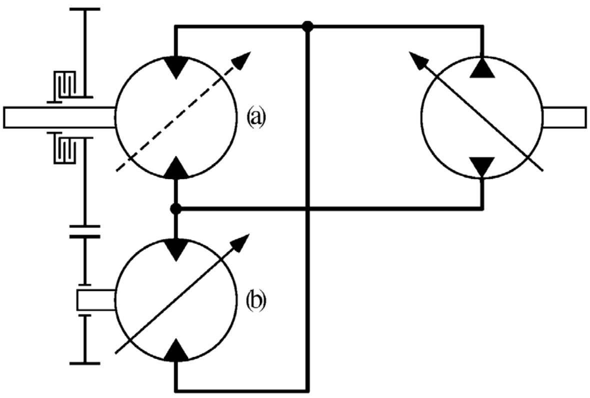

Figure 7. Scheme of the Type C/D transmission (with a disk clutch).

3.2. Application range

The pump and motor size are derived from Figure 3, provided that the actual power ratio be replaced by the virtual one R_i/u. Nevertheless, a word of caution is due because the x-coordinate of the size map is likely to be less than 5, which reduces the discriminating role of the motor and the confidence in the saturation of Ω. A countermeasure might be the unbalanced settings, i.e. to fix α_2 and derive $\alpha_1 = u/(\alpha_2 R_i)$; until $\alpha_1 \leq 1$ the pump boundaries become parallel to and higher than the motor boundaries.

If u is unrestricted, a gearbox with more than two steps would be able to negotiate almost any power ratio and substantial engine power; the top gear ratio would come from Equation (12) and then divided into the proper number of steps. In practice, cost as well as complexity would increase dramatically and the hydrostatic components would be more and more subsidiary to the mechanical components, ending up in some sort of series CVT without the advantages of a true parallel CVT.

3.3. Gear shift

The analysis of the shifting process is within neither the scope nor the space of the present paper, but a few remarks might be helpful to show that the HT changes the classical interaction between gearbox and engine.

The process is affected by the hardware. In Figure 4 the transmission features a double side synchronizer, actuated by a single external signal (left or right). The upshift and downshift last normally less than one second and are implemented by emulating a front clutch through proper control sequences in which the motor setting is also driven to zero (Klaas *et al.* 2012). If the motor is not a zero motor or the power flow is to be maintained during the shift – power shift – the transmission is provided with a pair of clutches, actuated by two coordinated signals, e.g. (Tolksdorf 1993). In all instances, the engine speed is insensitive to the gear shift.

4. Type C transmission

It is common sense that the potential of the HT might be expanded by more motors coupled to a summing box. Actually, the cooperation of two motors in parallel is exploited in systems ranging from low to high complexity. On the simple end, twin motors coupled to a fixed geometry gearbox either replace a larger and slower unit (e.g. from Table 1 two 60 motors accept the same maximum flow as one 160 motor) or double the application range (the motor boundaries of Figure 3 are shifted upwards); almost a replica of the Type A transmission with minor changes in the relevant equations. On the opposite end, two motors of different size and separate settings are coupled to a gearbox with more than two shiftable ratios as in Figure 6, derived and adapted from Rink (1994): the transmission features four operating ranges, three with both motors and one with a single motor. The hardware and software complexity makes schemes like this restricted to really demanding applications and their analysis a challenging task.

Somewhere in the middle stays the smart architecture of Figure 7, where the first motor (motor a) is always connected to the output shaft, and the second motor (motor b) is connected or disconnected; the displacement of motor b must be variable, while the displacement of motor a can be fixed or variable. At first, this class of transmissions was described in Leidinger (1992), Reinecke and Leidinger (1992) and subsequently implemented by others, e.g. Pfordt (1996), Kohmäscher (2011). It's not difficult to realize that the scheme of Figure 6 achieves a fruitful synergy between this principle and the Type B transmission.

The Type C transmission presumes motor a to have constant displacement, according to the early implementation known as 'Hydrotransmatic' transmission (Leidinger 1992), and its operation is in brief the

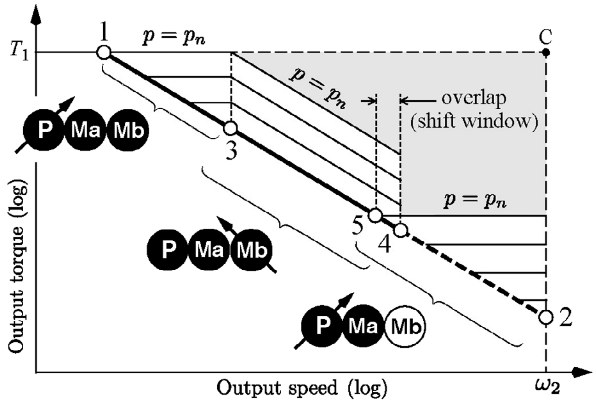

Figure 8. Mechanical characteristic of the Type C transmission (log-log scale).

Table 2. Key points of the Type C transmission (Figure 8).

Mode	Point	a_p	a_{ma}	a_{mb}	p	ω_{ma}	ω_{mb}
L	1	α_1	1	1	p_n	ω_1	$u\,\omega_{ma}$
	3	1		1	$\alpha_1 p_n$	ω_3	
	4	1		α_4	$\alpha_1 p_n$	ω_4	
H	5	α_1	1	0	p_n	ω_5	0
	2	1			$\alpha_1 p_n$	ω_2	

following. In the high torque or low speed (L) mode, both motors are connected to the output shaft and the setting of pump and motor b follow the sequential rule until the minimum setting of motor b is reached; in the low torque or high speed (H) mode, motor b is disconnected and motor a reaches its maximum speed. The shift between the two modes is actuated within a relatively small window by a tooth or disk clutch – in some implementations a one-way clutch (Ivantysynova and Weber 2006, Schubert 2007) – working within an epicyclic gear or a chain of spur gears. The mechanical package, much simpler than a gearbox, is conveniently integrated with the hydraulic units.

Few sources disagree on the architecture of Figure 7: in Marchand and Morize (1980), for instance, motor b reverses in the H mode to help the pump in supplying motor a, and in Dorgan and Wallace (1989) an epicyclic gear is driven in such a way that one motor only works in the L mode and both motors in the H mode (the opposite of Figure 7).

4.1. Properties and size

Supposed to be 1 the speed ratio of motor a and $u > 1$ the ratio of motor b, the ideal characteristic of the transmission has five key points divided in two groups (Figure 8): point 1, 3 and 4 in the L mode, point 5 and 2 in the H mode. The basic attributes of the key points are collected in Table 2, where the standby condition presumes motor b to be a zero motor.

The power ratio is defined as usual from the corner power in point C and the engine power corresponding to the hyperbola between point 1 and 2

$$R_i = \frac{p_n(D_a + uD_b)\omega_2}{P_e} = \frac{1 + uD_b/D_a}{\alpha_1} \qquad (15)$$

where uD_b is a sort of 'effective' displacement of motor b. Having three members, Equation (15) is equivalent to an algebraic system in the unknowns D_a and uD_b

$$D_a + uD_b = \frac{P_e R_i}{\omega_2 p_n} \qquad (16)$$

$$\frac{uD_b}{D_a} = \alpha_1 R_i - 1 \qquad (17)$$

Equation (16) explains how motors cooperate to increase the product $P_e R_i$, indicative of the application range; Equation (17) suggests that if R_i is moderately high the effective displacement of motor b is larger than the displacement of motor a.

Stated that the upstream constraints do not change and consequently the pump displacement replies Equation (6), by solving Equations (16) and (17) the displacement of motor a is

$$D_a = \frac{P_e}{\omega_2 p_n \alpha_1} \qquad (18)$$

The displacement of motor b takes a few more calculation steps, starting from the flow continuity in point 4 written as

$$\alpha_4 \omega_4 uD_b + (\omega_5 + \delta\omega_2)D_a = \omega_p D_p \qquad (19)$$

where $\delta\omega_2$ is the shift overlap range defined as in Equation (14). By plugging Equation (18) and the flow continuity in point 2 and 5 into Equation (19), the displacement of motor b is

$$D_b = \frac{P_e(1 - \alpha_1 - \delta)}{(u\omega_4)p_n \alpha_1 \alpha_4} \qquad (20)$$

where $u\omega_4$ is the actual speed of the motor. The speed ratio u is calculated from Equation (17).

The next step starts from the explicit calculation of the shift overlap range $\delta\omega_2 = \omega_4 - \omega_5$ from the output speed in point 4 and 5

$$\delta\omega_2 = \omega_p \frac{D_p}{D_a}\left[\frac{1}{\alpha_4 uD_b/D_a + 1} - 1\right] \qquad (21)$$

The proper substitutions bring to a peculiar relationship between the relevant settings α_1 and α_4, power ratio and overlap (peculiar because independent of pump and motors size)

$$[\alpha_4(\alpha_1 R_i - 1) + 1](\alpha_1 + \delta) = 1 \qquad (22)$$

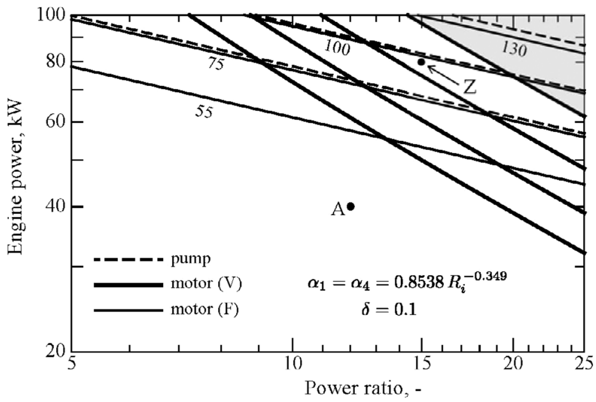

Figure 9. Size map of the Type C transmission (coupled settings).

By extracting α_4 and replacing it in Equation (20), the displacement of motor b eventually becomes

$$D_b = \frac{P_e(\alpha_1 R_i + \delta R_i - 1 - \delta/\alpha_1)}{(u\omega_4)p_n} \tag{23}$$

Between a priori specifications and a posteriori checks stays the measure of the operation range of motor a in the H mode, i.e. the relative ratio of transmission speed range λ between point 4 and 2, which is an extension of Equation (7)

$$\frac{\omega_2 - \omega_4}{\omega_2} = \lambda = 1 - \alpha_1 - \delta \tag{24}$$

In general λ should be neither too small (otherwise motor a would be of little help) nor too large (otherwise α_1 would become too small and detrimental to efficiency).

4.2. Application range

Given the specifications (R_i, P_e, δ) and a pre-specified value for p_n, the Type C transmission is described by the undetermined nonlinear system of five Equations (6), (17), (18), (22) and (23) with nine unknowns ω_p, ω_2, $u\omega_4$, α_1, α_4, D_p, D_a, D_b, u, four of which are in excess. Three degrees of freedom are removed immediately by expressing ω_p, ω_2 and $u\omega_4$ in proportion to the maximum speed of pump and motor a, and the top speed of motor b, respectively. Then, the size of the hydraulic units can be written with the same conventions of Section 2.3

$$D_{pj}^{1-\varepsilon_p} = \frac{P_e}{\varphi_{pj}\,\varpi_p p_n \alpha_1} \qquad j = 1, \ldots, 3 \tag{25}$$

$$D_{aj}^{1-\varepsilon_{mf}} = \frac{P_e}{\varphi_{aj}\,\varpi_{mf} p_n \alpha_1} \qquad j = 1, \ldots, 4 \tag{26}$$

$$D_{bj}^{1-\varepsilon_{mv}} = \frac{P_e(\alpha_1 R_i + \delta R_i - 1 - \delta/\alpha_1)}{\varphi_{bj}\,\varpi_{mv}\,\Omega(\alpha_4) p_n} \quad j = 1, \ldots, 4 \tag{27}$$

where the subscripts of φ are adapted to the new architecture, and the overspeed function Ω is presumably saturated, since α_4 is unlikely greater than 0.625. The speed ratio u is calculated from Equation (17).

The last degree of freedom to be removed is α_1 which has to be managed in conjunction with α_4 resulting that at least three methods are accessible to solve the sizing problem.

4.2.1. Coupled settings

This method assumes that $\alpha_1 = \alpha_4$ and consequently converts Equation (22) into a polynomial of degree 3 in α; by treating δ as a constant input (0.1 from here on) and R_i as a parameter ranging as in Figure 3, the solution is copied by a power law

$$\alpha_1 = \alpha_4 = 0.8538 R_i^{-0.349} \qquad 5 \le R_i \le 25 \tag{28}$$

The comparison between the corresponding size map (Figure 9) and Figure 3 reveals the dramatic restriction of the unfeasible region (grey), due to the ascent of the boundaries of motor b, that is still decisive to discriminate the feasibility; being dependent on α_1 linearly, the boundaries of pump and motor a are parallel each other.

Point A, feasible by a hair in Figure 3, now requires the smallest motors; conversely, point Z – capable of the considerable performance of $P_e = 80$ kW and $R_i = 15$ – requires the following minimum size hardware (design S_1 in brief, where pump and motors are identified by their labels for convenience)

$$S_1 \doteq [\mathrm{P} \equiv 100 \quad \mathrm{Ma} \equiv 100 \quad \mathrm{Mb} \equiv 160 \quad u = 2.48]$$

Within the same method, the effects of the relaxed coupling $\alpha_4 = k\,\alpha_1$ are explained by the opposite dependence on α_1 of Equations (25)–(27), discordant in pump and motor a, concordant in motor b: if $k < 1$ the motor b boundaries move down while the pump and motor a boundaries move up; if $k > 1$ the opposite movements are observed and the discrimination of feasibility tends to shift from motor b to motor a.

4.2.2. Decoupled settings

According to this method, α_1 and α_4 are chosen freely as long as they obey Equation (22). A good tool to do this is the map of Figure 10, where the solution of Equation (22) is plotted for some values of R_i; the upper limit of α_4 prevents the saturation of the overspeed function, while the lower limit breaks what stated in Table 1, as implied in Kohmäscher (2011), because the variable motor doesn't work alone.

Any couple (α_1, α_4) is acceptable, provided that the corresponding point lies on the relevant R_i = const curve; then, the pump and motor size are checked with simple operations on a spreadsheet based on Equations (25)–(27). In principle, this method could give good results; by selecting, for instance, $\alpha_4 = 0.2$

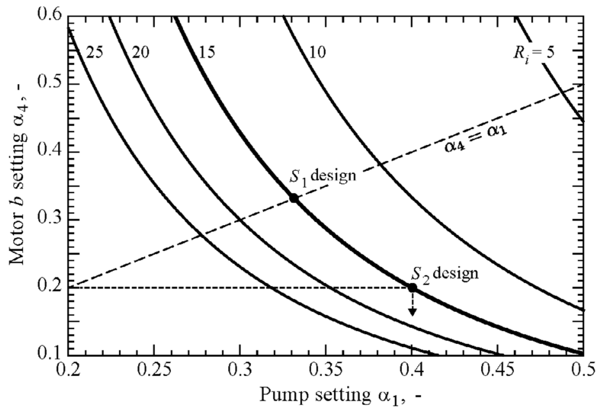

Figure 10. Map of the decoupled settings ($\delta = 0.1$).

Table 3. Sample of feasible triplets of Type C transmission (floating settings).

α_1	P	Ma	Mb	α_4	u
0.397–0.398	78	75	160	0.204–0.203	2.32–2.33
0.322–0.398	100	100	160	0.358–0.203	2.39–3.10
0.266–0.398	130	130	160	0.580–0.203	2.43–4.03
0.266–0.311	130	130	110	0.580–0.392	3.53–4.33

the specifications of point Z are satisfied by the following minimum size hardware (design S_2)

$$S_2 \doteq [\mathrm{P} \equiv 78 \quad \mathrm{Ma} \equiv 75 \quad \mathrm{Mb} \equiv 160 \quad u = 2.32]$$

Two units being smaller than in design S_1 is good, but both motors are on their boundaries and the pump is almost there (98% of its maximum speed).

4.2.3. Floating settings

It is arguable whether the previous methods be the proper help to the designer as both have a weak side: Figure 9 gives an overview of the transmission potential but suffers the stiff restraint on settings; Figure 10 gives more freedom but no overview of the results and forces a trial and error search.

A closer view discovers them to be partial simplifications of a general procedure that starts from Equations (25)–(27): given the specifications (P_e, R_i, δ), the following procedure applies to each possible triplet (D_p, D_a, D_b):

- Equations (25)–(27) are individually solved in α_1 by setting $\varphi_p = \varphi_a = \varphi_b = 1$ and $\Omega(\alpha_4) = \Omega_0$.
- The solutions α_{1p} from Equation (25) and α_{1a} from Equation (26) are lower limits of α_1, whereas the solution α_{1b} from Equation (27) is an upper limit of α_1 by virtue of the opposite dependence.
- The triplet is rejected if $\alpha_{1b} < \alpha_{1x} = \max\left\{\alpha_{1p}, \alpha_{1a}\right\}$. Otherwise.

(1) From the interval (α_{1x}, α_{1b}) of α_1 other intervals are calculated: α_4 through Equation (22), u through Equation (15), φ_p, φ_a and φ_b through Equations (25)–(27). The relative trends are always the same: $\alpha_1 \uparrow \alpha_4 \downarrow u \uparrow \varphi_p \downarrow \varphi_a \downarrow \varphi_b \uparrow$ and vice versa.

(2) The interval of α_4 is checked against a reference one, e.g. $0.1 \le \alpha_4 \le 0.625$ as in Figure 10. If the whole interval is outside, the triplet is rejected; if one extreme only is outside, it's rectified and α_1, u, etc ... are calculated again.

The specifications of point Z produce 10 triplets (none rectified); the four detailed in Table 3 have special meanings. The first is the same as in design S_2 and the smallest one; the second is the same as in design S_1; the third is the largest one; the fourth is something special, being the only one admitting Mb smaller than 160 and $D_a > D_b$ (reverse size configuration).

It is physically reasonable that as the main units become smaller the intervals of the design parameters decrease until collapsing to almost nothing, when at least two units reach the maximum speed or the top speed. If the interval is not negligible, the choice of a specific value is always a compromise because the relative trends and resultant effects on the efficiency of the main units are conflicting.

4.3. Gear shift

The transitions from L mode to H mode (upshift) and vice versa (downshift) should occur within the shift window (Figure 8) and completed only when necessary by introducing some hysteresis, e.g. upshift close to point 4 and downshift close to point 5. Connection and disconnection of motor b are tough tasks and their control has been addressed by a number of authors, e.g. (Sannelius and Palmberg 1995, Krauss and Ivantysynova 2003). Simple summaries are in Table 4 assuming that motor b be a zero motor – otherwise, an additional brake is needed – and the relevant sequence be mechanically or hydraulically actuated by a disk or tooth clutch, respectively.

All shifts are associated with pressure transients that determine their smoothness and consequently their duration (from few seconds to less than one second). Generally speaking the hydraulically driven downshift is the most critical sequence.

The gear shifting of the Type C transmission – and the following Type D as well – has a favourable impact on the final feeling to the driver. In fact, it does not suffer gaps in tractive effort over the full range, giving a feeling similar to torque converter transmissions with power-shift gearbox (a tough competitor in several applications), generally applied and well perceived in a large range of off road machines.

5. Type D transmission

The Type D transmission is an upgrade of Type C that presumes motor a displacement to be variable (Figure 7): the L mode does not change, the H mode becomes

Table 4. Summary of the shift sequences (Type C transmission).

	Disk clutch	Tooth clutch
Upshift	Motor *b* setting is moved to zero and pump setting is adjusted to maintain the speed of motor *a*; then the clutch is released while motor *b* is self-locking and does not affect the circuit	Motor *b* setting is decreased until its output torque vanishes, clutch is released at no load and setting is moved further to zero. Pump setting is adjusted to maintain the speed of motor *a*
Downshift	Intermediate clutch is engaged and accelerates motor *b* at zero setting until the clutch members are synchronized; then clutch is locked, motor setting moved up from zero, and pump setting adjusted accordingly	Motor *b* setting is increased from zero until output torque appears and its shaft is accelerated by the pump until the speed of the clutch members are synchronized and locked at no load

Table 5. Key points of the Type D transmission (partial).

Mode	Point	α_p	α_{ma}	α_{mb}	p	ω_{ma}	ω_{mb}
H	5	α_1	1	0	p_n	ω_5	0
	6	1	1		$\alpha_1 p_n$	ω_6	
	2	1	α_2		$\alpha_1 p_n$	ω_2	

a replica of the Type A transmission. In spite of appearances, the expectation of a simple superimposition of effects would be largely misleading.

5.1. Properties and size

The basic attributes of the key points in H mode are collected in Table 5, which replies the last rows of Table 2 with the addition of the intermediate point 6.

The updated power ratio is

$$R_i = \frac{p_n(D_a + uD_b)\omega_2}{P_e} = \frac{1 + uD_b/D_a}{\alpha_1\alpha_2} \tag{29}$$

If compared with Equation (15), two settings instead of one make the transmission able to negotiate higher power ratios; incidentally, the position $u = 0$ brings back to Equation (4) or Type A, and the position $\alpha_2 = 1$ brings back to Equation (15) or Type C.

The pump displacement is still given by Equation (6) because the interface with the prime mover doesn't change, while the displacement of motor *a* becomes

$$D_a = \frac{P_e}{\omega_2 p_n \alpha_{12}} \qquad \alpha_{12} = \alpha_1\alpha_2 \tag{30}$$

The displacement of motor *b* is found through the same procedure of Section 4.1 and its intermediate result is a relationship with strong similarities with Equation (22)

$$[\alpha_4(\alpha_{12}R_i - 1) + 1](\alpha_{12} + \delta) = \alpha_2 \tag{31}$$

The final displacement of motor *b* is as in Equation (23) provided that α_1 be replaced by α_{12}. The same applies to λ by transforming Equation (24).

5.2. Application range

By reasoning as in Section 4.2, the updated transmission model has five equations but ten variables instead of nine, five of which are in excess. The three degrees of freedom related with speed are removed in the usual way and the size of the hydraulic units become as follows

$$D_{p\,j=1,\ldots,3}^{1-\varepsilon_p} = \frac{P_e}{\varphi_{pj}\,\varpi_p p_n \alpha_1} \tag{32}$$

$$D_{a\,j=1,\ldots,4}^{1-\varepsilon_{mv}} = \frac{P_e}{\varphi_{aj}\,\varpi_{mv}\,\Omega(\alpha_2)p_n\alpha_{12}} \tag{33}$$

$$D_{b\,j=1,\ldots,4}^{1-\varepsilon_{mv}} = \frac{P_e(\alpha_{12}R_i + \delta R_i - 1 - \delta/\alpha_{12})}{\varphi_{bj}\,\varpi_{mv}\,\Omega(\alpha_4)p_n} \tag{34}$$

where $\Omega(\alpha_4)$ is more than likely saturated and the favorable effect of $\alpha_2 < 1$ is not immediately felt as in Equation (29). The speed ratio u is calculated from Equation (17) by replacing α_1 with α_{12}.

The last degrees of freedom to be removed are α_1 and α_2, in conjunction with α_4 through Equation (31). Since the coupled settings rule $\alpha_1 = \alpha_2 = \alpha_4$ is far too restrictive, three other methods are accessible to find a solution to the sizing problem.

5.2.1. Partly coupled settings

According to this method: first, the position $\alpha_2 = 0.625$ makes Equation (33) parallel to Equation (26) because $\Omega(\alpha_2)\alpha_2 = 1$; second, the reduced power ratio $R_i' = R_i\alpha_2$ and the augmented overlap $\delta' = \delta/\alpha_2$ make Equation (34) parallel to Equation (27); third, the surviving settings are coupled, i.e. $\alpha_1 = \alpha_4$. The second point is a clear proof of the advantage of Type D over Type C, which is confirmed graphically by the relevant size map (Figure 11).

The boundaries of motor *b* move up considerably, more than pump and motor *a*; consequently the minimum size units required to meet the specifications of point Z are (design S_3)

$$S_3 \doteq \left[P \equiv 100 \quad Ma \equiv 110 \quad Mb \equiv 80 \quad u = 3.37\right]$$

Partly better than design S_1 but what about S_2? Whichever judgement be made, the potential of the variable motors is not fully exploited, as proved by the relatively high settings ($\alpha_4 \approx 0.37$ and $\alpha_2 = 0.625$). As happens frequently in Type D transmissions, design S_3 features the reverse size configuration, which is prevented to all but one Type C transmissions.

The comparison of the size maps of Figures 3, 9 and 11 is easier if the top boundaries of the relevant transmissions

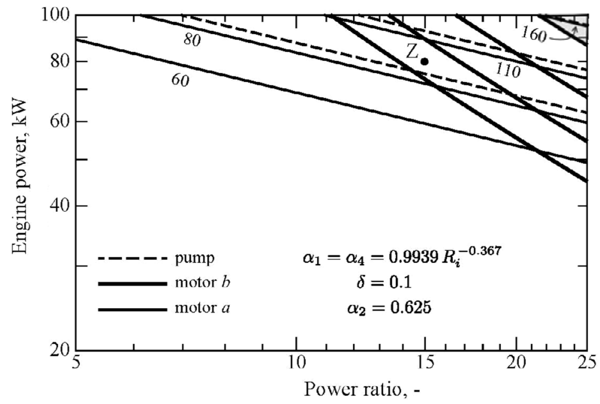

Figure 11. Size map of the Type D transmission (partly coupled settings).

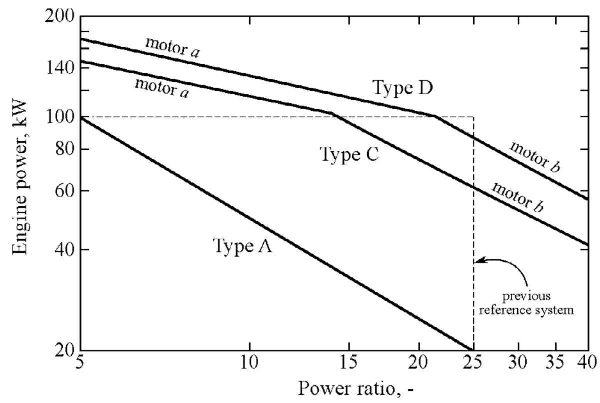

Figure 12. Comparison of the size maps (Type A, C and D).

Table 6. Sample of triplets with decoupled settings (Type D transmission).

α_1	P	Ma	Mb	α_4	u
0.495–0.497	78	60	110	0.144–0.143	1.99–2.00
0.409–0.497	78	80	110	0.267–0.143	2.06–2.66
0.390–0.406	78	110	80	0.308–0.273	3.65–3.86
0.331–0.406	100	110	80	0.494–0.273	2.89–3.86

Table 7. Variants of the triplet 78-110-60 (floating settings).

α_2	α_1	α_4	u	φ_p
0.625		(Interval of α_1 incompatible)		
0.500	0.413–0.426	0.300–0.271	3.85–4.03	0.94–0.91
0.400	0.517–0.533	0.145–0.126	3.85–4.03	0.75–0.73
0.300	0.537–0.541	0.106–0.100	3.77–3.83	0.73–0.72
0.250		(Interval of α_4 incompatible)		

are plotted in the same reference system, broader than the previous one for convenience (Figure 12). It is worth remarking that this is surely the best of Type A, while Type C and D can resort to much better methods though unsuitable for a simple graphical translation.

5.2.2. Decoupled settings

This method combines the position $\alpha_2 = 0.625$ with the procedure of Section 4.2.3 by replacing Equations (25)–(27) with Equations (32)–(34). The improvement over the first method is dramatic.

The specifications of point Z produce 34 feasible triplets, 15 of which rectified; differently from Type C, motor b is never 160. For illustration purposes, four triplets are detailed in Table 6: the first three are the smallest ones; the fourth is the same as in design S_3.

The comparison between the second and the third triplet is interesting because they exchange the same motors but the effect on the relevant parameters is considerable.

5.2.3. Floating settings

This method makes a further step by applying the procedure of Section 5.2.2 to decreasing values of α_2, which implies the saturation of $\Omega(\alpha_2)$ in Equation (33).

An interesting result of tests run with the specifications of point Z is the increase of the rectified triplets: if $\alpha_2 = 0.5$ the gross total is 30 (22 of which rectified), if $\alpha_2 = 0.3$ all 12 triplets are rectified. For illustration purposes, Table 7 shows what happens to the same triplet by decreasing α_2 from 0.625 to 0.250 and in particular: firstly, the interval of u is partially insensible because it depends on α_{12} i.e. the size of motors; secondly, the decrease of α_2 permits a decrease of the pump speed, favorable to efficiency without increasing the pump size.

6. Efficiency

The past exposition of all HT schemes went from a set of specifications, e.g. R_i, P_e, δ (Type C or D), to a set of design parameters, e.g. D_p, D_a, D_b, u, α_2, α_4, φ_p (Type D), and its fluency was favored by the omission of the flow and torque losses in hydraulic units. Actually, an alternative formulation of the relevant models would be possible, inclusive of efficiency, but they would become intricate and implicit; for example, the power ratio of the Type D transmission would be, instead of Equation (15),

$$R_i = \frac{\eta_{vp}(2)\,\eta_{va}(2)\,\eta_{hp}(1)\,\eta_{ha}(1)}{\alpha_1\alpha_2}\left[1 + \frac{u D_b\,\eta_{hb}(1)}{D_a\,\eta_{ha}(1)}\right] \quad (35)$$

where $\eta_{va/b}(i)$ and $\eta_{ha/b}(i)$ are the volumetric and hydromechanical efficiency in point i of the mechanical characteristic; since they depend on setting (if applicable), pressure and speed (Paoluzzi and Zarotti 2013), the appreciation of interconnections and constraints would be irremediably lost. And the workaround of imposing constant efficiencies would be more confusing than helpful.

But sooner or later the efficiency should be involved in a well-structured design process meant to offer a closer estimation of the transmission performance. Without attempting such an approach, that would be the acceptable subject of a separate investigation, the following case studies aim to disclose how losses influence the characteristic of few sample transmissions.

Table 8. Design parameters of the case studies (Type C and D transmissions).

	P	Ma	Mb	u	φ_p	α_2	α_4	u_f
#1	78	75	160	2.322	0.973	–	0.200	18.9
#2	78	60	110	1.988	0.772	0.625	0.140	30.0
#3	78	110	60	4.000	0.725	0.400	0.126	24.0

7. Case studies

Three case studies of Type C and Type D transmissions are considered with the same specifications: engine power of 80 kW, power ratio of about 15 (ideal), shift overlap of 10% (ideal). For the purposes of technical communication the torque vs. speed curve is often converted into a proportional traction vs. speed curve, though the result be largely conventional because it lacks a vehicle model. Such a dummy machine, compatible with the machines mentioned at the beginning of the paper, is supposed to reach the maximum speed of about 40 km/h with a wheel diameter of 0.6 m by adding a final reduction u_f; the possible front reducer or multiplier to match engine and pump speed is not relevant to the analysis. A sure advantage of the dummy vehicle is the compensation of the different speed of motor a in point 2 of the characteristic.

The complete sets of design parameters are collected in Table 8: the first row (case #1) replies design S_2; the second row (case #2) complies with the first row of Table 6; the third row (case #3) complies with the third row of Table 7.

Some numbers are rounded for convenience and consequently the ideal performance does not match exactly the specifications: actually, the power ratio is 14.83/14.69/14.77, and the overlap is 10.1/9.8/9.8. The maximum speed is always 42.4 km/h (11.8 m/s), a conservative target.

7.1. Numerical results

The coordinates of a generic point of the traction vs. speed curve are given by two relationships subject to the constraints on input power $P_e = \text{const} = \omega_p \alpha_p D_p p / \eta_{hp}$ and input speed $\omega_p = \text{const}$. As to the Type D transmission (Type A and C are easily derived by putting $u = 0$ and $\alpha_a = 1$), they are

$$F = \frac{u_f\, \alpha_a D_a p\, \eta_{ha}}{r}\left[1 + \frac{u D_b}{D_a}\frac{\alpha_b}{\alpha_a}\frac{\eta_{hb}}{\eta_{ha}}\right] \tag{36}$$

$$v = \frac{r P_e \eta_p \eta_{va}}{u_f\, \alpha_a D_a p}\left[1 + \frac{u D_b}{D_a}\frac{\alpha_b}{\alpha_a}\frac{\eta_{va}}{\eta_{vb}}\right]^{-1} \tag{37}$$

where $\eta_p = \eta_{vp}\eta_{hp}$ is the total pump efficiency. By multiplying the above equations the transmission efficiency due to the main hydraulic units is

$$\frac{Fv}{P_e} = \eta_p \eta_a \left[1 + \frac{u D_b}{D_a}\frac{\alpha_b}{\alpha_a}\frac{\eta_{hb}}{\eta_{ha}}\right]\left[1 + \frac{u D_b}{D_a}\frac{\alpha_b}{\alpha_a}\frac{\eta_{va}}{\eta_{vb}}\right]^{-1} \tag{38}$$

where $\eta_a = \eta_{va}\eta_{ha}$ is the total efficiency of motor a. The volumetric and hydromechanical efficiency come either from closed form models – as, for instance, in Paoluzzi and Zarotti (2013) – or from the interpolation of numerical arrays. To be consistent with the decision of Section 2.2 to adopt discrete series of units, the data base originated by a renowned manufacturer is used: 360 points to map the variable pump, 544 the variable motor, and 80 the fixed motor. The interpolation is done by two- and three-dimensional routines based on the algorithm described in Renka (1988) and called by a dedicated software developed by the authors. In the common L mode, for instance, the calculations are: (a) find by iteration the pressure in point 3 (pressure in point 1 is known); (b) find by iteration the pump setting and the output speed in the intermediate points between 1 and 3; (c) find by iteration the output speed in the intermediate points between 3 and 4.

The traction vs. speed curves of the dummy vehicle – opposed to the ideal curve (dotted) – and the efficiency plots are in Figure 13, where the key points are labeled as usual.

7.2. Comparisons

One way of comparing the results of Figure 13 is to look at what is in some way related to the key points. The geometric appearance is that from case #1 to case #3 the H range increases (λ changes from 51 to almost 69%), the shift window moves to the left, and the maximum speed slightly decreases. Other quantitative parameters are in Table 9. The power ratio is not far from the target – actually 93.5/91.3/89.7% – and contradicts the statement found in some literature that the total efficiency of the main units affect the ideal power ratio (see also Equation (35)). More distant from the target is the overlap δ, which is not bad because some margin is left to refine the design. As to the speed ranges, the pump speed decreases strongly from Type C to Type D, which is good for the efficiency, while more critical is motor a for it sustains the rotation from point 1 to point 2 and the designer should pay attention no to cross the lower limit stated by the manufacturer; this is a weak side of both Type C and D transmission because the overall speed range is intrinsically limited and the data of Table 9 seem quite close to such a limit.

Another way of comparing the results of Figure 13 is to look at the efficiency plots. The average calculated in the portions of the characteristics delimited by the key points is found in Table 10, with the efficiency in point 2 added for convenience. Since the functional dependence of the efficiency is always the same, the results could be explained by a deeper analysis, e.g. the difference in pump speed (see Table 9) and minimum pressure ($p_3/p_n = 0.355, 0.480, 0.515$ from case #1 to case #3).

In the L range the Type D transmissions are better than Type C; in the H range the averages reward case

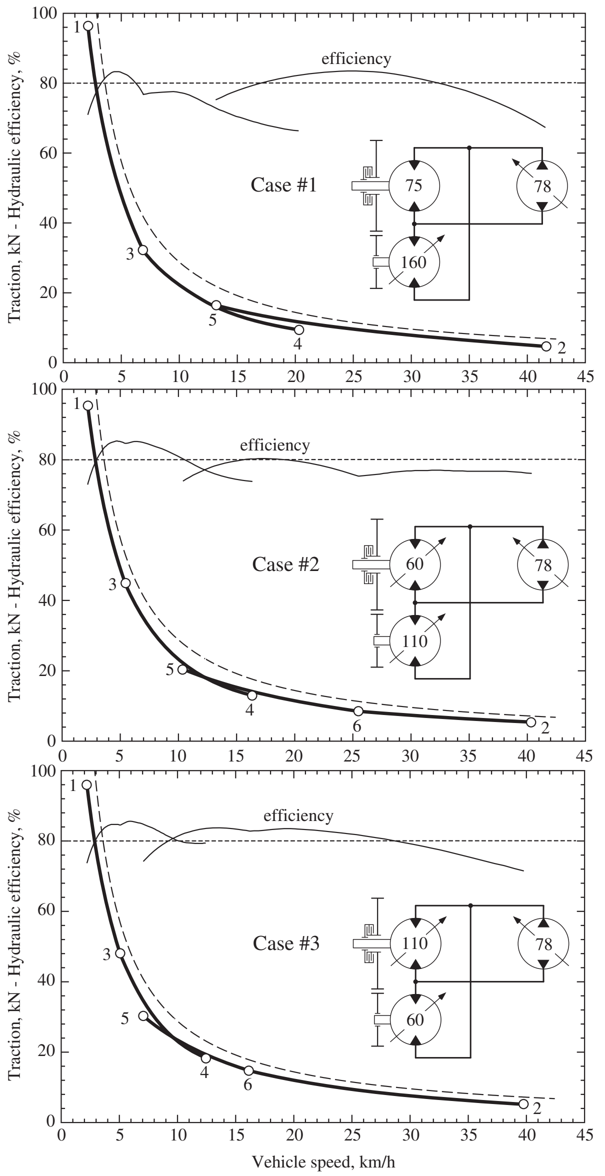

Figure 13. Traction and efficiency vs. speed of the three case studies.

Table 9. Relevant parameters of the numerical case studies.

	R_i	δ (%)	ω_p/ω_n	ω_a/ω_n^* Min	ω_a/ω_n^* Max	ω_b/ω_n^* Min	ω_b/ω_n^* Max
#1	13.87	17.0	0.973	0.080	0.969	0.262	1.517
#2	13.41	14.8	0.772	0.050	1.492	0.168	1.471
#3	13.25	13.5	0.725	0.081	1.440	0.197	1.470

*The maximum speed of variable motors refers to full setting.

Table 10. Average efficiency along the mechanical characteristic, (%).

	L range			H range		
	1–3	3–4	5–2	5–6	6–2	point 2
#1	79.7	73.0	79.2	–	–	67.4
#2	81.7	79.7	–	78.3	76.5	76.1
#3	81.5	82.1	–	81.2	80.2	71.5

#3, followed by case #1 and case #2, though case #2 is more flat and largely the best at the top speed. It's also interesting that the ratio $\eta/(\eta_p\eta_a)$ in Equation (38), which is one by definition in the H mode, exceeds one in the L mode under 6 km/h in Type C and 3.5 in Type D. Though such results reveal that the favorable influence on the efficiency is a primary criterion to screen the feasible triplets, any ranking based on math only is not conclusive since an effective evaluation would require the efficiency plots be multiplied by a weighting function derived from the working cycle/s of the machine: e.g. the probability of working in the shift window is likely low and, according to the chief engineer of a leading telehandler manufacturer, the probability of working at high torque is greater than working at high speed.

7.3. Flexibility

Sometimes the engines are instructed to run at lower speed to increase the fuel efficiency, and the speed ranges of the transmission should decrease more or less proportionally. But the Type D transmissions, differently from Type C, feature the ability to compensate the effect by further decreasing the setting of motor *a* in point 2 and reach almost the maximum speed anyway. The control of the input torque should be treated with care – keep it constant or take advantage of the torque margin of the engine – because the overlap decreases. The same opportunity is open to the Type B transmissions, provided that α_2 had some margin left; the effect on the overlap is questionable.

8. Conclusions

A major development driver of the hydrostatic packages for wheeled machine locomotion is the expansion of their application range – combination of power ratio and engine power – to challenge fierce mechanical competitors.

Beside improving the simplest HT (one pump and one motor) with a shiftable two-step gearbox, in recent years a simpler architecture emerged, based on two motors, one of which is connected to or disconnected from the output shaft.

To estimate the potential of the candidate transmission schemes their constitutive models must be compatible with the discrete series of pumps and motors commercially available.

The design data (size of units, extreme settings and gear ratio if pertinent) result from sizing methods, which are relatively complex and scarcely intuitive in the multi-motor schemes. Surprisingly, the number of possible combinations of the main units offered by the most general procedures – the floating settings – is rather large if compared with the few alternatives of the simple HT with gearbox. It means that the multi-motor schemes are worthy of further investigations because their potential is likely yet to be exploited.

Note

1. The fixed motor is not considered because the aim of the paper is to show the maximum potential of the scheme with two units.

Disclosure statement

No potential conflict of interest was reported by the authors.

Nomenclature

D	Cubic displacement of pumps and motors, m^3/rad
F	Vehicle tractive effort, N
P	Power, W
Q	Volume flow rate in hydraulic lines, m^3/s
R	Power ratio, –
T	Shaft torque of pumps and motors, Nm
p	Differential pressure of the hydraulic lines, Pa
r	Radius of the vehicle driving wheels, m
t	Time, s
u	Gear ratio, –
v	Vehicle speed, m/s
Ω	Overspeed function of motors, –
A	Displacement setting of pumps and motors, –
δ	Shift overlap ratio of adjacent operating modes, –
η	Efficiency of pump and motors, –
λ	Relative ratio of transmission speed range, –
ω	Shaft speed of pumps and motors, rad/s
ε	Power law exponent (series of pumps and motors), –
φ	Speed divided by maximum (pumps) or top (motors) speed, –
ϖ	Power law coefficient (series of pumps and motors)
	Subscripts
a, b	First and second motor
e	Engine
f	Fixed or final
h	Hydromechanical
i	Internal
m	Motor
n	Maximum
p	Pump
v	Variable or volumetric

Notes on contributors

Roberto Paoluzzi, born in Ferrara in 1961, received the degree in Nuclear Engineering from the University of Bologna in 1986. Since 1988 he joined the Institute for Agricultural and Earthmoving Machines of the National Research Council of Italy (CNR). From 2009 until his sudden death on September 13th 2016, he was the director of the same Institute from 2002 to 2009. Main interests in the field of fluid power transmission, computational fluid dynamics and functional analysis of the safety of machinery. He is the author or co-author of over 200 scientific publications, he was the teacher at the University of Modena and Reggio Emilia, and University of Ferrara. He was an associated editor of the "International Journal of Fluid Power". Vice Secretary-General ISTVS (International Society for Terrain-Vehicle Systems) for EMEA. Chairman of the Technical Committee ISO / TC 127 SC4 (Earth Moving Machinery - Terminology, commercial nomenclature, classification and ratings).

Luca G. Zarotti, born on November 20th 1945 in Parma, he received the Degree in Aeronautical Engineering at the Polytechnic Institute of Torino (1970). In 1971, he joined the Institute for Agricultural and Earthmoving Machines of the National Research Council of Italy (CNR), where he is still working. He was the director of the same Institute from 2002 to 2009. He had in charge the fluid power course at the Polytechnic Institute of Torino (from 1979 to 1982) and the University of Modena & Reggio E. (from 1996 to 1999), and the University of Ferrara (from 2002 to 2012). His research interests cover various aspects of hydrostatic locomotion, displacement control of pumps and motors, load sensing and flow sharing systems for mobile applications. Besides a number of papers and articles, he is the author of Monographs on fluid power fluids (2006), Fluid power circuits (2006 and 2010) and Hydrostatic transmissions (2010). Retired at the end of 2012, he still works on fluid power projects with the Institute as an associate researcher.

ORCiD

Roberto Paoluzzi http://orcid.org/0000-0001-5857-5972

References

Dorgan, R.J. and Wallace, D.A., 1989. *Dual hydrostatic drive transmission*. US patent 4848186.

Ivantysynova, M. and Weber, J., 2006. *Hydrostatic multi-motor drive*. US patent 2006/0162329A1.

Klaas, H., Mejia, F., and Riggenmann, F., 2012. Don't stop – shift on fly. *Proceedings conference for mobile applications MOBILE 2012, RE 00207/10.2012*, Bosch Rexroth, Ulm, Germany.

Kohmäscher, T., 2011. Multi-motor transmissions – increased transmission ratio to support advanced control systems. *Proceedings 52nd national conference on fluid power*. NFPA, 113–124.

Krauss, A. and Ivantysynova, M., 2003. Control concept for a multiple-motor type hydrostatic transmission. *Proceedings 18th international conference on hydraulics and pneumatics*. Prague, 183–194.

Leidinger, G., 1992. Hydrotransmatic – Ein neuartiger stufenloser, lastschaltfreier hydrostatischer Fahrantrieb [Hydrotransmatic - A new loss free, power shift hydrostatic transmission]. *Ölhydraulik und Pneumatik*, 36, 222–232.

Marchand, D. and Morize, A., 1980. *Transmissions hydrostatiques de puissance è grande plage de fonctionnement* [Hydrostatic power transmission with large operational rang]. EP patent 0026115A2.

Paoluzzi, R. and Zarotti, L.G., 1997. About the minimum transmission size. *In:* Burrows C.R. and Edge K.A., eds. Fluid power systems. *Ninth Bath International Fluid Power Workshop*. 954-968, Bath, England: Research Studies Press. ISBN 0863802109.

Paoluzzi, R. and Zarotti, G.L., 2013. The minimum size of hydrostatic transmissions for locomotion. *Journal of terramechanics*, 50, 153–164.

Pfordt, H., 1996. *Dual hydraulic motor drive system*. US patent 5518461.

Reinecke, U. and Leidinger, G., 1992. *Infinitely variable hydrostatic transmission drive*. US patent 5159992.

Renka, R.J., 1988. Multivariate interpolation of large sets of scattered data. *ACM transactions on mathematical software (TOMS)*, 14, 139–148.

Rink, S., 1994. Hydraulische Antriebsysteme für Radlader groß er Leistung, *Proceedings 11th Aachener Fluidtechnisches Kolloquium, Verein zur Förderung der Forschung und Anwendung der Hydraulik und Pneumatik* [Hydrostatic transmission for more powerful wheel loader] Band (2), 55–71.

Rydberg, K.-E., 1997. *Hydrostatic drives in heavy mobile machinery – new concepts and development trends. SAE paper 981989*. Warrendale, PA: Society of Automotive Engineers.

Sannelius, M. and Palmberg, I.O., 1995. Control aspects of hydrostatic transmissions with sequence-controlled motors. *Proceedings fourth Scandinavian international conference on fluid power*. Tampere University of Technology, Tampere, Finland, 1073–1086.

Schubert, M., 2007. *Getriebevorrichtung für ein Kraftfahrzeug und Kraftfahrzeug* [Transmission device for a motor vehicle and motor vehicle]. EP patent 1983230A1.

Tolksdorf, D., 1993. *Elektro-hydraulische Steuerung für lastschaltbare Getriebe in Fahrzeugen* [Electrohydraulic control for variable-load motor vehicle transmission]. DE patent 4340126A1.

Zarotti, L.G. and Paoluzzi, R., 1996. In quest of the transmission size. *Proceedings of the JFPS international symposium on fluid power*, 1996 (3), 295–300. doi: http://dx.doi.org/10.5739/isfp.1996.295.

Appendix

Zero motor

For a long time a myth spread throughout the fluid power community: avoid the zero setting of variable motors, otherwise the speed will run away. Actually, an acceleration takes

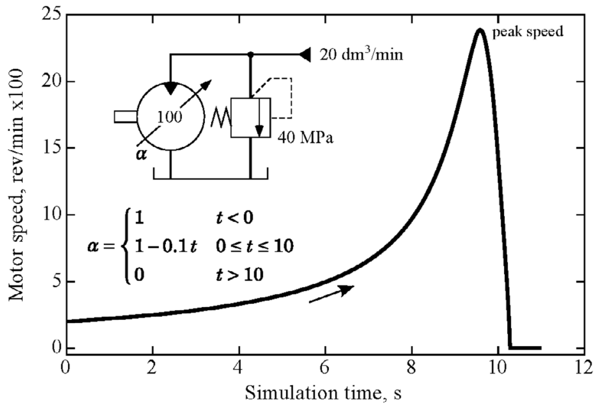

Figure A1. Transient of a variable motor while its setting is forced to zero.

place but this is not the end of the story: in fact, the motor accelerates until the active torque (proportional to fluid pressure and setting) is greater than the passive torque due to friction, but when the inequality reverses the acceleration becomes negative. To see what happens, a virtual experiment can be useful. The simulated speed of an unloaded variable motor – modeled more or less as in Paoluzzi and Zarotti (2013) and supplied by a constant flow source with a relief valve in parallel – subject to a decreasing setting from one to zero is plotted in Figure A1 and confirms the qualitative description above plus something more; once stopped, the motor is self- locking and an external torque is necessary to rotate it again. This is the feature of interest in transmission design, irrespective of whether a real motor sustains the peak speed or not.

The boundary conditions of the experiment of Figure A1 are for demonstration only and the interaction of the motor with a more complex environment would be hard to appreciate by qualitative reasoning, but the basic principle is not contradicted.